Emotion Recognition from Multidimensional Electroencephalographic Signals On the Manifold of Symmetric Positive Definite Matrices

Eman A. Abdel-Ghaffar
Electrical Eng. Dept., Faculty of Eng. Shoubra, Benha Univ., Cairo, Egypt
eman.mohamed@feng.bu.edu.eg

Mohamed Daoudi
IMT Lille Douai, Univ. Lille, CNRS UMR 9189 CRIStAL, Lille, France
mohamed.daoudi@imt-lille-douai.fr

Abstract

The aim of this study is to classify human emotions using Electroencephalographic (EEG) signals. The main contribution of our approach is classifying four classes of emotions using a simple distance metric Log-Euclidean Riemannian Metric (LERM) on a symmetric positive definite manifold (SPD). In this work, four classes of emotions were recognized (HVHA, LVHA, LVLA, and HVLA) using four different channel combinations (2-channels, 7-channels, 10-channels, and 18-channels) over four frequency bands (theta, alpha, beta, and gamma). Our approach shows comparable results to existing studies applied on the DEAP dataset. The best emotion classification accuracy for HVHA is 88.3%*, LVHA is* 84.38%*, LVLA is* 79.3%*, and HVLA is* 78.4%*. The average recognition accuracy for valence is* $74.6\% \pm 3.9$*, and* $72.6\% \pm 6.7$ *for arousal.*

1. Introduction

Emotions plays a vital role in human communication, most human computer interaction (HCI) systems are still not efficient in understanding emotions. Human emotion state can be extracted either through voice [5], facial expressions [8], Electroencephalography (EEG) signals, or combining multiple modalities for a more accurate system [24]. In multimedia systems, emotion identification is very important in determining the effects of different multimedia materials, and EEG based emotion identification is growing attention in this area [21][22]. Various techniques for feature extraction from EEG signals have been used in the literature including, time domain techniques [20], frequency domain techniques [18] [23][15][29], joint time-frequency analysis techniques [19][9]. The use of symmetric positive definite manifold for EEG based classification problems is relatively new, but it is spreading quickly and is currently applied in various applications including image processing, radar data processing, medical imaging, computer vision, machine learning, and brain-computer interaction [4] [6].

In this paper, four class emotion classification system is developed based on using Log-Euclidean Riemannian Metric (LERM) on a symmetric positive definite manifold. Emotion classification from multi-channel EEG signals in DEAP dataset was studied using four different channel combinations and over four different frequency bands.

2. Related Work

Most emotion recognition techniques based on EEG signals, extract features either from time domain or frequency domain or joint time and frequency domains. In time domain the variation of the EEG signal time series is studied and from which features are extracted. Statistical features (Energy, Power, Entropy, Mean, Standard deviation, etc.) have been used extensively [19][20].

In frequency domain techniques, time domain EEG signal is transformed into frequency domain using Fast Fourier Transform (FFT) or one of its alternatives (Shot-Time Fourier Transform (STFT), Discrete Wavelet Transform (DWT)). The most common frequency feature is Power Spectral Density (PSD) generated from different sub-bands (Delta 0-4 HZ, Theta 4-8 HZ, Alpha 8-16 HZ, Beta 16-32 HZ, and Gamma 32-64 HZ)[23]. Thammasan et al. [26] and Zheng et al. [29] used frequency domain features (Fractal dimension, Power spectral density) for emotion classification.

Due to the non-stationary nature of the EEG signals, new techniques combining time and frequency domain were introduced to capture new features. In [9] Hadjidimitriou et al. extracted Hilbert-Huang Spectrum (HHS) energy and

978-1-7281-4272-2/20/$31.00 ©2020 IEEE
DOI 10.1109/MIPR49039.2020.00078

Authorized licensed use limited to: Middlesex University. Downloaded on August 31,2020 at 18:12:39 UTC from IEEE Xplore. Restrictions apply.

use it to study music liking for different individuals. Li et al. [13] studied EEG signals in both time and frequency domains using Hilbert-Huang transform (HHT). The use of Riemannian geometry in EEG signal analysis and in brain-computer interaction (BCI) is attracting more researchers because of its robustness, accuracy, and simplicity. Cogedo et al. [6] offered a complete review on the use for Riemannian geometry for EEG-based brain computer interaction.

The rest of this paper is organized as follows; In section 3, we consider the EEG signal recorded from N electrodes as covariance matrices and we study the Riemannian geometry of the SPD manifold and the the classification approach. Experimental results and discussions are reported in section 4 . In section 5, we conclude and draw some perspectives of the work. The full approach is illustrated in Fig. 1.

3. Methodology

3.1. The SPD manifold

Consider the EEG signal recorded from N electrodes, each electrode signal forms a single time series $x_i(t)$ where $i = 1, ...N$,. Each time domain signal is divided into small windows (in this work we used 4 sec. with 50% overlap), this results in 28 windows. Convolution is performed between each window and the corresponding windows coming from the N electrodes to generate 28 covariance matrices $C_i, i = 1, .., 28$. We denote by $X \in \mathbb{R}^{N\times n}$ a given EEG recording epoch recorded from N electrodes and having n samples per window. The covariance matrix C between N random variables is a square matrix $C \in \mathbb{R}^{N\times N}$ [6] given by:

$$C = \frac{1}{N-1} XX^T \tag{1}$$

3.2. Riemannian geometry of Symmetric positive-definite matrices

A non-singular covariance matrix C of size $N \times N$ belongs to the set of symmetric positive-definite (SPD) matrices. These do not form a vector space (the space is not closed under matrix subtraction), rather they form a connected Riemannian manifold Sym_N^+ [6]. As such, the distance between SPD matrices is not accurately captured by the Euclidean distance. Several distance measures on Sym_d^+ have been proposed. The most widely used is the Log-Euclidean Riemannian Metric (LERM) [6]. Given two SPD matrices C_i and C_j, their LERM distance is computed as:

$$\delta_2(C_i, C_j) = \|log\left(C_i^{\frac{-1}{2}} C_j C_i^{\frac{-1}{2}}\right)\|_F \tag{2}$$

where $\|\cdot\|_{\mathrm{F}}$ is the Frobenius norm operator.

The geometric mean between SPD matrices can be generated using various techniques [7][3], three of those approaches are used in this study. The cheap mean (CM) [7] is defined by;

$$(C_1, C_2, ..., C_m) = exp\left(\frac{1}{m}\sum\nolimits_{i=1}^{m} log\,(C_i)\right) \tag{3}$$

The Geometric mean between two matrices (GM1) [7][3] is defined by;

$$C_i \# C_j = C_i^{\frac{1}{2}}\left(C_i^{\frac{-1}{2}} C_j C_i^{\frac{-1}{2}}\right)^{\frac{-1}{2}} C_i^{\frac{1}{2}} \tag{4}$$

and the Geometric mean between m matrices(GM2) [7][3] is defined by;

$$\left(\left(\left(\left(C_1 \#_{\frac{1}{2}} C_2\right) \#_{\frac{1}{3}} C_3\right) \#_{\frac{1}{4}} C_4\right) \ldots \#_{\frac{1}{M}} C_M\right) \tag{5}$$

Where ;

$$C_i \#_t C_j = C_i^{\frac{1}{2}}\left(C_i^{\frac{-1}{2}} C_j C_i^{\frac{-1}{2}}\right)^t C_i^{\frac{1}{2}} \tag{6}$$

3.3. Emotion Model

In this study, we use a two dimensional emotion model of valence and arousal for classifying four classes of emotions (HVHA, LVHA, LVLA, and HVLA). valence shows the degree of delight and varies from negative to positive. Arousal shows the degree of emotion activation and varies from excitement to calm. Figur 2 shows the valence-arousal dimension model of human emotion.

3.4. Emotion Classification

Let $\left\{\left(C^{(1)}, l^{(1)}\right), \ldots, \left(C^{(n)}, l^{(n)}\right)\right\}$ be a training set of labeled samples. Where for each $1 \leq i \leq n$, $C^{(i)}$ is a covariance matrice and $l^{(i)}$ is the corresponding emotion labels, $l^{(i)} \in \{e_1, e_2, e_3, e_4\}$ in a certain frequency band, and coming from N electrodes. Our goal is to find a function that associates an element of Sym_d^+ its classification label $l^{(i)} \in \{e_1, e_2, e_3, e_4\}$. In Euclidean spaces, any standard classifier (e.g. standard SVM) may be a natural and appropriate choice to classify Euclidean data. Unfortunately, this is no more suitable as the space Sym_d^+ is non-linear. In this paper following the idea of [1], we propose to compute the mean $\widehat{C}(l)$ of each emotion covariances class e_i by using one of the geometric described above during the training phase. The classification is based on an minimum distance by using the Log-Euclidean Riemannian Metric (LERM) d_{LERM} between unknown SPD matrix and the mean. To

Authorized licensed use limited to: Middlesex University. Downloaded on August 31,2020 at 18:12:39 UTC from IEEE Xplore. Restrictions apply.

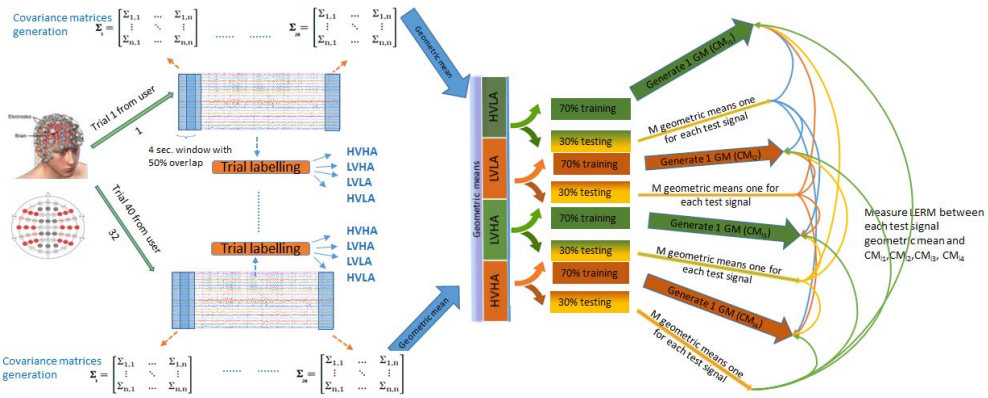

Figure 1: Emotion brain computer interaction cycle starting from capturing the EEG signals from multiple electrodes, dividing it into small 4 sec. 50% overlapping windows, generating covariance matrices, labeling the signal to one of four emotion states, generating the geometric mean for each trial covariance matrices.

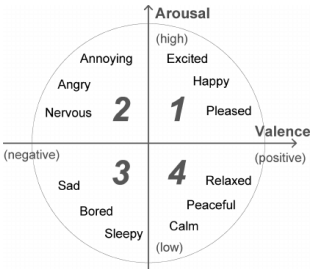

Figure 2: valence-Arousal model of human emotion.

be more precise, given l classes and a training phase where the mean is defined by $\widehat{C}(l)$, a new observation Ci is assigned to the class l according to the classification rule

$$\widehat{l} = \arg \min_{l \in \{e_1, e_2, e_3, e_4\}} \left\{ d_{LERM} \left(C_i, \widehat{C}(l) \right) \right\} \quad (7)$$

4. Experimental Results

4.1. Dataset

DEAP dataset [11] consists of the multi-channel EEG signals of 32 individuals (16 women and 16 men, with average age 26.9) recorded while watching 40 one-minute videos. The EEG signals were recorded using 32 electrodes and sampled at 512 HZ. The electrodes were arranged according to the international 10-20 positioning system [16][10].

In this work, we are using the preprocessed version of the dataset in which; The data was down sampled to 128 sample/sec., EOG artifacts were removed, the data was averaged to the common reference and was filtered using a base band frequency filter from 4.0 - 45.0 HZ.

4.2. Temporal windowing

In DEAP dataset the EEG acquisition time is 60 seconds, which is longer than the recognition time of emotion states. For accurately identifying the emotion state, EEG signals are divided into short segments by windowing. In [25] Thammasan et al. tested the performance of emotion recognition with window duration that varies from 1 to 8 seconds their result showed that the smaller the window size the higher the performance. In [17] Mohammadi et al. stated that the emotion hold time is from 2 to 4 sec. and found that 4 sec. windows yield better performance. Through this work we used a window size of 4 seconds with 50% overlap.

4.3. Channel selection

In DEAP data set EEG signals are recorded from electrodes placed according to the international 10-20 system [16] shown in Figure (3). In our approach we study emotion classification based on EEG signals recorded from 2 channels, 7 channels, 14 channels, and 18 channels. Those channel configurations were selected based on the experience of other researchers [12][14]. The two channels are; F3-F4. The 7 channels are; P3, P7, PO3, O1, PZ, C4, and CP2. The 10 channels are; F3-F4, F7-F8, FC1-FC2,FC5-FC6, and FP1-FP2. 18 channels are composed of the 10 channels plus AF3-AF4, C3-C4, T7-T8, and FZ-CZ.

4.4. Emotion Classification Labels

In DEAP dataset, there exist 32 subjects in each subject file there exist two arrays, one for the 32 electrodes time domain signals and one for the labels. Participants were asked to label each trial by rating the levels (giving a score

Authorized licensed use limited to: Middlesex University. Downloaded on August 31,2020 at 18:12:39 UTC from IEEE Xplore. Restrictions apply.

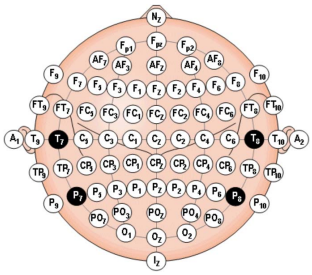

Figure 3: The international 10-20 system. A = Ear lobe, C = central, Pg = nasopharyngeal, P = parietal, F = frontal, Fp = frontal polar, O = occipital. [16]

Table 1: Emotion Classification Labels.

Emotion Label	Scores	Number of Samples
HVHA	$V \geq 5, A \geq 5$	458
LVHA	$V < 5, A \geq 5$	297
LVLA	$V < 5, A < 5$	260
HVLA	$V \geq 5, A < 5$	265
Total		1280

between 1 and 9) of arousal, valence, liking and dominance for each of the 40 one-minute long music videos.

According to the given scores of valence (V) and arousal (A), we divided the two dimensional emotion plane into four classes. Table (1) clarify the labels, the valence and arousal scores used for labeling, and the number of samples in the dataset that belongs to each label. Using score 5 as a threshold is taken in this research in order to be able to compare our performance with other researchers [17][28]. By using threshold, we treat the classification problem as four class binary classification problem.

4.5. Results and Discussion

In this work we studied the emotion classification problem from different angles. Emotion recognition accuracy for EEG signals recorded from different channel combinations were studied for 2 channels, 7 channels, 10 channels, and 18 channels. We study the classification accuracy of the emotion states on the original EEG signals without frequency separation, then on different frequency bands (theta (4-8 HZ), alpha (8-16 HZ), beta (16-32 HZ), gamma (32-45 HZ)).

Classification between four different classes of emotions HVHA, LVHA, LVLA, and HVLA were carried out. This was done using three methods for computing the geometric mean cheap mean (CM), geometric mean between two matrices (GM1), and geometric mean between m matrices (GM2).

Due to the large set of results we obtained, we summarized our results and the best accuracy achieved for the 4 classes classification problem is shown in table 2, along with the frequency band and the geometric mean generation method. The best accuracy for HVHA emotion state (excited, happy, pleased) was 88.3%, LVHA emotion state (annoying, anger, nerves) was 84.38%, LVLA emotion state (sad, board, sleepy) was 79.3%, and HVLA emotion state (relaxed, peaceful, calm) was 78.4%.

We found that most existing studies on DEAP dataset classify emotions into two classes valence (Positive/Negative), arousal (Pleasant/Unpleasant). For comparing our classification accuracy with these studies, the mean and standard deviation accuracy for valence and arousal of our approach is shown in table 3. A comparison between the accuracy achieved using our approach and other studies is shown in table 4. The results achieved are comparable to other more complex and time consuming approaches [17][27][14][2][28].

5. Conclusion

In this paper we have classified four classes of emotions, using four different EEG channel combinations, working on the original signal without frequency separation and four other frequency bands, and using three different methods for computing the geometric mean. The best emotion classification accuracy for HVHA is 88.3%, LVHA is 84.38%, LVLA is 79.3%, and HVLA is 78.4%. The average recognition accuracy for valence is $74.6\% \pm 3.9$, and $72.6\% \pm 6.7$ for arousal. In future work, we will focus on improving the labeling approach to take into consideration the liking and dominance scores and on trying different classification rules.

6. Acknowledgment

This study was supported by the French government through the Programme Investissement d'Avenir (I-SITE ULNE / ANR-16-IDEX-0004 ULNE) managed by the Agence Nationale de la Recherche.

References

[1] A. Barachant, S. Bonnet, M. Congedo, and C. Jutten. Multiclass brain-computer interface classification by riemannian geometry. *IEEE Trans. Biomed. Engineering*, 59(4):920–928, 2012.

[2] O. Bazgir and et al. Emotion recognition with machine learning using EEG signals. *25th National and 3rd International Iranian Conference on Biomedical Engineering (ICBME)*, November 2018.

Authorized licensed use limited to: Middlesex University. Downloaded on August 31,2020 at 18:12:39 UTC from IEEE Xplore. Restrictions apply.

Table 2: The classification results with different channel combinations and methods for the four emotion classes.

Emotion	2-channels			7- channels			10-channels			18-channels		
Label	Acc.	Freq.	Method	Acc.	Freq.	Method	Acc.	Freq.	Method	Acc.	Freq.	Method
HVHA	47%	all	CM	61.1%	alpha	GM2	67.5%	theta	GM2	88.3%	theta	GM2
LVHA	66%	all	GM1	82.7%	all	GM2	77.8%	gamma	GM2	84.4%	alpha	GM2
LVLA	79.3%	all	GM1	58%	gamma	CM	50.5%	alpha	GM1	58.34%	all	CM
HVLA	78.4%	alpha	GM1	76.84%	beta	GM1	73.88%	theta	GM1	74.44%	beta	GM1

Table 3: The classification results valence and arousal with different channel combinations and methods.

	2 Channels valence Accuracy					2 Channels Arousal Accuracy				
Method	all signal	Gamma	Beta	Alpha	Theta	all signal	Gamma	Beta	Alpha	Theta
CM	56.8 ±1.3	59.7 ±2.3	55 ±0.9	54.3 ±2.7	58 ±4	52.65 ±5.5	54.35 ±7.65	50.2 ±5.7	51.1 ±6.9	50.3 ±7.7
GM1	57.95 ±12.3	60.8 ±12	62.1 ±11.8	74.6 ±3.9	59.6 ±17	72.6 ±6.7	64.75 ±8.35	65 ±8.8	55.25 ±13.5	69. ±7.9
GM2	53.55 ±18.5	59.85 ±17	58.25 ±3.75	52.15 ±3.75	58.5 ±12	68.55 ±9.15	68.54 ±6.15	67.85 ±6.85	58.85 ±2.95	66.7 ±3.8
	7 Channels valence Accuracy					**7 Channels Arousal Accuracy**				
Method	all signal	Gamma	Beta	Alpha	Theta	all signal	Gamma	Beta	Alpha	Theta
CM	60.3 ±10.3	60.65 ±12.15	63.1 ±11.6	55 ±0.45	61.55 ±10.05	61.8 ±8.8	65.4 ±7.4	65.4 ±9.3	53.45 ±1.95	64 ±7.6
GM1	64.5 ±8.7	58.65 ±8.85	63.25 ±13.65	61 ±14.5	62.4 ±6.1	60.35 ±12.8	58.6 ±8.6	63.55 ±13.35	64.9 ±10.6	60.5 ±8
GM2	67.65 ±15	52.7 ±2.8	60.55 ±14.2	57.3 ±11	57.3 ±7.3	64.55 ±16	51.35 ±4.15	63 ±11.7	64.65 ±3.55	52.3 ±14.1
	10 Channels valence Accuracy					**10 Channels Arousal Accuracy**				
Method	all signal	Gamma	Beta	Alpha	Theta	all signal	Gamma	Beta	Alpha	Theta
CM	57.9 ±6	56.4 ±4.5	56.85 ±5	54.15 ±8.45	57.55 ±5.75	61 ±2.85	58.35 ±2.55	59.1 ±2.8	61.5 ±4	60.9 ±2.4
GM1	51.25 ±2.65	58.55 ±10	56.13 ±13	60.9 ±10.4	55.65 5 ±12.25	52.85 ±1.05	60.5 ±0.1	64.75 ±4.65	61.65 ±9.65	68.5 ±5.85
GM2	50.35 ±1.65	67.05 ±10.85	62.7 ±4.2	53.2 ±2.8	50.95 ±10	48.7 ±1	61.95 ±15	54.85 ±12	53.55 ±3.15	69.4 ±1.9
	18 Channels valence Accuracy					**18 Channels Arousal Accuracy**				
Method	all signal	Gamma	Beta	Alpha	Theta	all signal	Gamma	Beta	Alpha	Theta
CM	57.95 ±0.45	56.65 ±1.75	59.75 ±1.95	60.05 ±1.7	59.45 ±1.75	55 ±2.5	56.45 ±1.95	58.25 ±3.45	58.6 ±3.6	57.2 ±4
GM1	55.75 ±2.65	59.65 ±9.6	61.95 ±12.5	50.55 ±10.5	64.1 ±8	52.8 ±5.6	58.9 ±10.4	64.45 ±10	52 ±0.6	71.7 ±11
GM2	56.15 ±2.1	63.8 ±7.5	65.2 ±9.8	68.45 ±15	70.55 5 ±7.75	51.85 ±2.45	58.55 ±2.7	63.7 ±1.3	66.8 ±8.3	67.3 ±11

[3] R. Bhatia. *Matrix Information Geometry*, chapter 2. Springer, 2012.

[4] G. Chen. Digital riemannian geometry and its application. *In proceeding of 2nd International Conference on Advances in Computer Science and Engineering (CSE 2013)*, pages 279–283, 2013.

[5] J. Cho and et al. Deep neural networks for emotion recognition combining audio and transcripts. *Interspeech*, 49:247–251, November 2019.

[6] M. Congedo and et al. Riemannian geometry for EEG-based brain-computer interaction; a primer and a review. *Brain-Computer Interfaces*, 4(3):155–174, 2017.

[7] A. Dario and et al. A note on computing matrix geometric means. *Advances in Computational Mathematics*, 35:175–192, November 2011.

Authorized licensed use limited to: Middlesex University. Downloaded on August 31,2020 at 18:12:39 UTC from IEEE Xplore. Restrictions apply.

Table 4: Comparison between results of Various Emotion Classification Techniques.

Study	Year	Subjects	Domain	Classification Method	Accuracy
[27]	2016	32	2 classes valence and Arousal	CNN+RNN	74.12%
[14]	2017	32	4 classes valence and Arousal	CNN+LSTM RNN	75.21%
[17]	2017	32	2 classes valence and Arousal	K-NN	86.7%
[2]	2018	32	2 classes valence and Arousal	K-NN, SVM,NNT	valence 91.1% Arousal 91.3%
[28]	2018	32	2 classes valence and Arousal	CNN+LSTM RNN	valence 90.8% Arousal 91.03%
Our approach		32	4 classes valence and Arousal	Reimannian Geometry (Min-Distance to Mean)	valence 74.6% ±3.9 Arousal 72.6% ±6.7

[8] S. Griffiths and et al. Impaired recognition of basic emotions from facial expressions in young people with autism spectrum disorder: Assessing the importance of expression intensity. *Information Fusion*, 49:2768–2778, March 2019.

[9] S. Hadjidimitriou and et al. Toward an EEG-based recognition of music liking using time-frequency analysis. *IEEE Transactions on Biomedical Engineering*, (59):3498–3510, 2012.

[10] V. Jurcak and et al. 10/20, 10/10, and 10/5 systems revisited: Their validity as relative head-surface-based positioning systems. *Neuroimage*, 4(4):1600–1611, February 2007.

[11] S. koelstra and et al. Deap: A database for emotion analysis using physiological signals. *IEEE Transactions on Affective Computing*, 3(1):18–32, January 2012.

[12] M. Li and et al. Emotion recognition from multichannel EEG signals using k-nearest neighbor classification. *Technology and health care*, 26:509–519, 2018.

[13] X. Li and et al. An improved multi-scale entropy algorithm in emotion EEG features extraction. *Journal of Medical Imaging Health Information*, (7):436–439, 2017.

[14] Y. Li and et al. Human emotion recognition with electroencephalographic multidimensional features by hybrid deep neural networks. *Applied Sciences*, 7(10), October 2017.

[15] Y. Liu and et al. EEG-based dominance level recognition for emotion-enabled interaction. *IEEE International Conference on Multimedia and Expo, Melbourne, Australia*, page 1039–1044, July 2012.

[16] J. Malmivuo. *Bioelectromagnetism*, chapter 13, pages 247–264. Oxford University Press, 2012.

[17] Z. Mohammadi and et al. Wavelet based emotion recognition system using EEG signal. *Neural computing and applications*, 28(8):1985–1990, August 2017.

[18] M. Murugappan and et al. Classification of human emotion from EEG using discrete wavelet transform. *Biomedical Science Eng.*, 3:390–396, 2010.

[19] M. Murugappan and et al. Inferring of human emotional states using multichannel EEG. *European Journal of Scientific Research*, (2):281–299, 2010.

[20] D. Nie and et al. EEG-based emotion recognition during watching movies. *5th International IEEE/EMBS Conference on Neural Engineering, Cancun, Mexico*, page 667–670, May 2011.

[21] A. Raheel and et al. Emotion recognition in response to traditional and tactile enhanced multimedia using electroencephalography. *Multimedia tools and applications*, 78:13971–13985, November 2019.

[22] S. Siddharth and et al. Impact of affective multimedia content on the electroencephalogram and facial expressions. *Scientific Reports*, (16295), November 2019.

[23] M. Soleymani and et al. Valence-arousal evaluation using physiological signals in an emotion recall paradigm. *IEEE International Conference on Systems, Man and Cybernetics, Montreal, QC, Canada*, page 2662–2667, October 2007.

[24] M. Soleymani and et al. Analysis of EEG signals and facial expressions for continuous emotion detection. *IEEE Transactions on Affective Computing*, 7(1):17–28, January 2016.

[25] N. Thammasan and et al. Application of deep belief networks in EEG-based dynamic music emotion recognition. *International joint conference on Neural Networks*, July 2016.

[26] N. Thammasan and et al. Continuous music-emotion recognition based on electroencephalogram. *IEICE Transactions on Information and Systems*, E99-D(4):1243–1241, April 2016.

[27] L. Xiang and et al. Emotion recognition from multichannel eeg data through convolutional recurrent neural network. *IEEE International Conference on Bioinformatics and Biomedicine (BIBM), China*, page 352–359, December 2016.

[28] Y. Yang and et al. Emotion recognition from multi-channel EEG through parallel convolutional recurrent neural network. *International Joint Conference on Neural Networks (IJCNN)*, July 2018.

[29] W.-L. Zheng and et al. Multimodal emotion recognition using eeg and eye tracking data. *36th Annual International Conference of the IEEE Engineering in Medicine and Biology Society, Chicago, IL, USA*, pages 5040–5043, August 2014.

Authorized licensed use limited to: Middlesex University. Downloaded on August 31,2020 at 18:12:39 UTC from IEEE Xplore. Restrictions apply.